Geophysical Research Letters

RESEARCH LETTER
10.1029/2023GL104678

Microstructural Controls on the Uniaxial Compressive Strength of Porous Rocks Through the Granular to Non-Granular Transition

Lucille Carbillet[1], Fabian B. Wadsworth[2], Michael J. Heap[1,3], and Patrick Baud[1]

[1]Institut Terre et Environnement de Strasbourg, Université de Strasbourg, CNRS UMR, Strasbourg, France, [2]Department of Earth Sciences, Science Labs, Durham University, Durham, UK, [3]Institut Universitaire de France (IUF), Paris, France

Key Points:

- Deformation micromechanism changes from grain crushing (granular, high porosity) to pore-emanated cracking (non-granular, low porosity)
- A regime diagram provides the expected deformation micromechanism for clastic rock with a known porosity and grain size
- Micromechanical models provide strength estimates for clastic rock based on the micromechanism (grain crushing or pore-emanated cracking)

Supporting Information:

Supporting Information may be found in the online version of this article.

Correspondence to:

L. Carbillet,
lcarbillet@unistra.fr

Citation:

Carbillet, L., Wadsworth, F. B., Heap, M. J., & Baud, P. (2023). Microstructural controls on the uniaxial compressive strength of porous rocks through the granular to non-granular transition. *Geophysical Research Letters*, *50*, e2023GL104678. https://doi.org/10.1029/2023GL104678

Received 30 MAY 2023
Accepted 23 OCT 2023

Author Contributions:

Conceptualization: Lucille Carbillet, Fabian B. Wadsworth, Michael J. Heap, Patrick Baud
Data curation: Lucille Carbillet, Patrick Baud
Formal analysis: Lucille Carbillet, Fabian B. Wadsworth, Michael J. Heap, Patrick Baud
Funding acquisition: Michael J. Heap, Patrick Baud
Investigation: Lucille Carbillet, Fabian B. Wadsworth, Michael J. Heap, Patrick Baud
Methodology: Lucille Carbillet, Michael J. Heap, Patrick Baud

Abstract Under uniaxial compression, a porous rock fails by coalescence of stress-induced microcracks. The micromechanical models developed to analyze uniaxial compressive strength data consider a single mechanism for the initiation and propagation of microcracks and a fixed starting microstructure. Because the microstructure of clastic porous rock transitions from granular to non-granular as porosity decreases during diagenesis, their strength cannot be captured by a single model. Using synthetic samples with independently controlled porosity and initial grain radius we show that high-porosity granular samples, where microcracks grow at grain-to-grain contacts, are best described by a grain-based model. Low-porosity non-granular samples, where microcracks grow from pores, are best described by a pore-based model. The switch from one model to the other depends on porosity and grain radius. We propose a regime plot that indicates which micromechanical model may be more suitable to predict strength for a given porosity and grain radius.

Plain Language Summary Porous rocks can be characterized in terms of the proportion of empty spaces in them, that is, their "porosity." When porous rocks are compressed, small cracks can form and propagate inside the solid rock between the pores until they unite into a large fracture, leading to rock failure. Depending on the initial shape and arrangement of pores within the rock, the small cracks may form and grow in different locations and/or directions. To explore the variety in the formation and growth of cracks, we prepared artificial samples with varying porosity and grain sizes. We found that rocks with large porosity and grain-like structures break differently than rocks with low porosity and non-grain-like structures. In the first type, cracks grow and radiate from the connections between grains, while in the second type, cracks grow from the edge of pores toward the solid surroundings. Since differences in the location and manner in which cracks grow can result in variations in rock strength, we showed how different models may be needed for accurate strength prediction, depending on the porosity and grain size of the rocks.

1. Introduction

Across all geological settings, sediments are shaped by diagenetic processes operating at the grain scale that drive microstructural deformation and densification. During diagenesis, the microstructure evolves from an initially granular or clastic material to a dense and coherent rock, thus changing not only in porosity, but also in pore lengthscales and pore-phase topology (Doyen, 1988). This evolution involves a continuous shift from connected pore space between packed grains (a microstructure dominated by individual particles surrounded by pore fluid), to a porous, coherent, and indurated sedimentary rock (a microstructure dominated by individual pores surrounded by a solid continuum). The transition from the "granular" state to the "non-granular" end-state can be described as an inversion of the pore-phase topology (Wadsworth et al., 2017).

If we take uniaxial compressive strength (UCS) as a measure for brittle rock strength, it is clear that strength is dominantly controlled by porosity (Guéguen & Boutéca, 2004; Paterson & Wong, 2005). However, large UCS data sets show a substantial spread in strength for a given porosity and lithology (Baud et al., 2014, 2017; Chang et al., 2006; Zhu et al., 2011, 2016). This spread is typically attributed to compositional (e.g., clay and cement content) and microstructural differences (e.g., pore and grain size and shape). While numerical approaches can help in the effort to deconvolve microstructural attributes and porosity (Griffiths et al., 2017; McBeck et al., 2019; Peng et al., 2017; Scholtès & Donzé, 2013; Yu et al., 2018), they are often limited to two-dimensions, and are rarely used to scrutinize analytical predictive models.

Supervision: Michael J. Heap, Patrick Baud
Validation: Fabian B. Wadsworth, Michael J. Heap, Patrick Baud
Visualization: Lucille Carbillet, Fabian B. Wadsworth
Writing – original draft: Lucille Carbillet
Writing – review & editing: Lucille Carbillet, Fabian B. Wadsworth, Michael J. Heap, Patrick Baud

Micromechanical models have been proposed to interpret rock brittle strength data (Kemeny & Cook, 1991). The pore-emanated crack model (PECM; Sammis & Ashby, 1986), which provides a micromechanical description for the evolution of strength with porosity for a constant pore size, is one of the most frequently used models to analyze the deformation and failure of variably porous rocks (Baud et al., 2014; Wong & Baud, 2012). However, the PECM assumes a fixed microstructural state—circular voids with a constant radius embedded in a solid continuum (i.e., a non-granular microstructure)—and does not therefore consider the shift from a granular to non-granular microstructure as porosity is reduced. This may explain why the predictive capability of this type of model is often restricted to a certain porosity range (Wu et al., 2000).

Here, we explore this issue using new UCS data from synthetic samples in which we can control the microstructural elements and the porosity independently (cf., Carbillet et al., 2021). Granular synthetic samples are characterized by a high porosity and interconnected pore space while non-granular synthetic samples have a low porosity and isolated pores. We suggest that, instead of using a single model to describe mechanical behavior over the full range of porosity, a grain-based model is more appropriate to interpret UCS data at high porosity whilst a pore-based model is more appropriate for low porosity data. We found that the transition in deformation micromechanism occurs at a threshold porosity which depends on mean grain size. Finally, we propose a regime plot that indicates which micromechanical model may be most suitable to model the strength of a clastic rock of a given porosity and grain size.

2. Materials and Methods

Synthetic samples made of sintered glass beads were used in this study. Viscous sintering allowed us to prepare samples with porosities between 0.06 and 0.36 and microstructures representative of different degrees of granular densification (Wadsworth et al., 2016), following the protocol provided in Supporting Information S1 (Text S1). We embrace the philosophy outlined in Carbillet et al. (2021) in which the first-order mechanics of clastic rocks are understood to be well-approximated by systems of variably sintered size-controlled glass beads, while acknowledging that second-order effects, such as cement or a polymineralic nature of some clastic rock types, are not well captured by this synthetic system. Cylindrical samples (20 mm in diameter and 40 mm in length) were prepared by sintering monomodal and broadly monodisperse distributions of silicate glass spheres following the procedure detailed in Carbillet et al. (2021). Four different distributions were used, with mean grain radii of approximately 24, 112, 262, and 601 μm. The total porosity of each sample was calculated using their dimensions and mass and the solid density of the glass beads.

The UCS of the synthetic samples was measured on 55 dry samples loaded using an axial steel piston displaced at a constant servo-controlled rate corresponding to an axial strain rate of 10^{-5} s^{-1}. The displacement of the axial piston was monitored by an external linear variable differential transducer, which was then used to compute the axial strain of the samples. A load cell recorded the axial force, which was converted into the axial stress using the sample cross-sectional area. In order to better understand the micromechanisms of deformation, selected samples were jacketed with 0.1 mm-thick copper jackets to preserve their integrity following deformation. Those samples were impregnated with epoxy under vacuum post-deformation and then prepared into thin sections, which were observed using a scanning electron microscope (SEM) in backscatter mode.

3. Results: Porosity and Grain Size Controls

3.1. Mechanical Data

A representative stress-strain curve for a uniaxial test on a synthetic sample with a porosity of 0.11 is presented in Figure 1a. Additional mechanical data showing experimental repeatability are presented in Supporting Information S1 (Figure S1). When a synthetic sample is deformed under uniaxial compression, the stress-strain curve typically shows three domains (Figure 1a), similar to data reported for natural rocks, including sandstones (Baud et al., 2014): (a) the elastic domain, during which strain increases linearly with stress—sometimes preceded by a non-linear elastic phase attributed to the reorganization of grains by rotation and sliding—(b) the inelastic domain, during which microcracks initiate, propagate and coalesce and (c) the failure domain, during which the stress reaches a peak value (σ_u, the UCS of the rock) as coalesced micro-

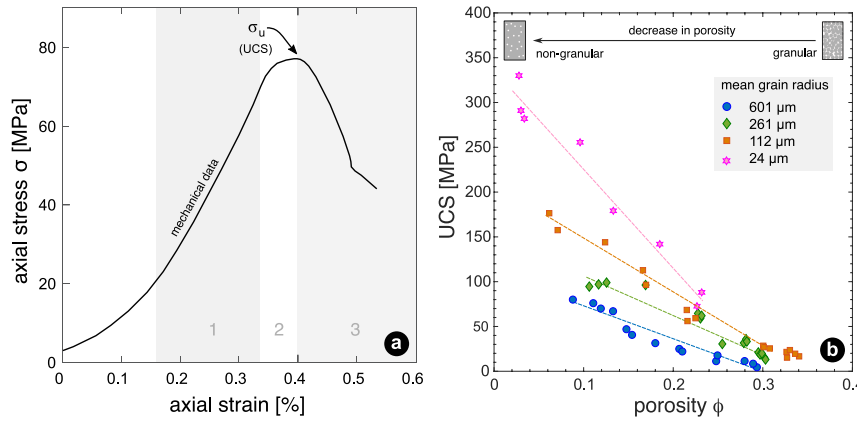

Figure 1. Representative mechanical data for the axial stress change with axial strain during uniaxial deformation. (a) Data presented are for a synthetic sample with $R = 601$ μm and $\varphi = 0.11$. The peak stress at brittle failure is marked σ_u. (b) Evolution of the uniaxial compressive strength (UCS) with porosity, for samples of different mean grain radius (indicated in the legend). The mean variation in UCS observed for repeated tests is approximately 6%. For reference, the UCS of a sample of pure soda-lime silica glass (porosity of 0%) is 617 MPa (Vasseur et al., 2013).

cracks form a localized shear fracture that signals the failure of the sample. Plots of UCS as a function of porosity, for samples with mean grain radius from 24 to 601 μm, are presented in Figure 1b. Broadly speaking, the strength of the synthetic samples is inversely correlated to porosity, suggesting that the decrease in porosity that accompanies granular densification leads to strength increase. For example, for synthetic samples with a mean grain radius of 24 μm, UCS increases from 88 to 330 MPa as porosity decreases from 0.23 to 0.03. For a constant porosity, an increase in grain radius results in a decrease in UCS. For example, for synthetic samples with a porosity of 0.13, increasing the mean grain radius from 24 to 601 μm decreases UCS from 179 to 67 MPa.

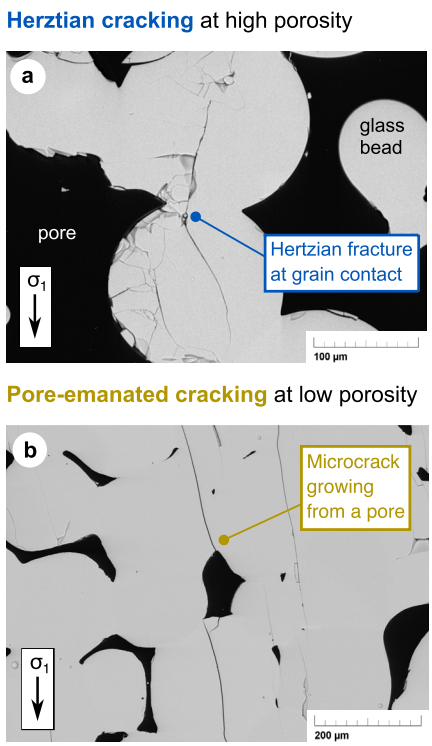

Figure 2. Microstructural deformation features under uniaxial compression. Scanning electron micrographs of samples with a (a) high and a (b) low porosity deformed up to the peak stress. (a) The microstructure shows that microcracks initiate at grain-to-grain contacts and form Hertzian fractures in poorly sintered samples with a high porosity and a microstructure close to granular. (b) In highly sintered samples, with a low porosity and a microstructure close to non-granular, pore-emanated microcracks grow from the poles of pores.

3.2. Microstructural Observations

All synthetic samples deformed under uniaxial compression failed in a brittle manner. However, different deformation features at the grain-scale were observed depending on the sample porosity. SEM images of synthetic samples deformed up to the peak stress are presented in Figure 2. Additional images are provided in Supporting Information S1 (Figures S2 and S3). We discriminate between the synthetic samples with a microstructure close to granular packing, that typically have a high porosity and within which adjacent spherical glass beads are interconnected by necks (Figure 2a), and those with a non-granular microstructure, that typically have a low porosity and isolated pores (Figure 2b). At high porosity, microcracks are found to have developed in the form of radiating fans originating at grain-to-grain contacts (Figure 2a). Within highly damaged areas, the length of microcracks forming these so-called Hertzian fractures reaches the diameter of the grains which then become comminuted. At low porosity, microcracks have grown from the boundary of pores in a direction parallel to the applied stress. In highly damaged areas, the microcracks coalesce into larger fractures. Contrary to the wide spatial distribution of damage in high-porosity synthetic samples, damage anisotropy is obvious in the low-porosity samples where pore-emanated cracks develop. We further note that, because microcracks are restricted to the diameter of the grains, they are shorter in the high-porosity samples than in the low-porosity samples.

4. Micromechanical Modeling

Under uniaxial compressive stress, rocks fail by the coalesce of microcracks to form a macroscopic fracture. To predict rock strength, it is critical to understand how and from where individual microcracks initiate and propagate. Based on experimental observations, micromechanical models have been developed for the analysis of damage evolution in porous rocks. Sammis and Ashby (1986) derived the PECM which belongs to the "inclusion" model family, and considers a microstructure idealized as an elastic continuum within which isolated equant pores are embedded. As a macroscopic uniaxial stress is applied to this system, the model is predicated on the computation of stress concentration at the surface of spherical pores. When the cumulative stress intensity factor reaches a critical value, K_{IC}, tensile microcracks nucleate from the poles of the pores and propagate parallel to the direction of the maximum principal stress, σ_1. Pore-emanated microcracks grow stably as σ_1 increases, until the growth of the pore cracks becomes unstable, at which state they coalesce into a macroscopic fracture along which the sample fails. The PECM provides a simple micromechanical framework for the analysis of the influence of porosity, φ, and pore radius, r, on the UCS, σ_u. The full solution of the PECM requires a numerical approach, and so Zhu et al. (2010) proposed an analytical approximation of the form

$$\sigma_u = \frac{1.325}{\varphi^{0.414}} \frac{K_{IC}}{\sqrt{\pi r}}. \quad (1)$$

At low porosity, the synthetic samples used in this study show a microstructure dominated by spherical pores, similar to that considered in inclusion models such as the PECM. Moreover, our microstructural observations show pore-emanated cracks in low-porosity samples (Figure 2). Therefore, using the mechanical properties of our soda-lime silica glass beads in Equation 1, we can compare our mechanical results to the predictions of the PECM as a function of porosity. Studying the same family of controlled sintered glass samples as dealt with here, Vasseur et al. (2017) proposed to replace the pore radius r with $l_1(\varphi)$ the inter-particle distance in a porous medium (Torquato, 2002). Here, we follow this rationale and replace the pore radius in Equation 1 by the inter-particle distance, computed using $l_1(\varphi) = R[\Gamma(4/3)\eta^{-1/3}]$ where Γ is the gamma function and $\eta = -\ln(1-\varphi)$. This approach is crucial because it provides a lengthscale for the pores—approximated as the inter-particle lengths—for all porosities, as a function of the known initial particle radii only.

At high porosity, the synthetic samples show a microstructure dominated by spherical grains that differs from the initial microstructure considered in the PECM. However, although "granular" micromechanical models that consider an initial microstructure modeled as an assembly of contacting elementary particles with known dimensions (e.g., spherical grains) in a given packing arrangement have been proposed, they have not been used to describe brittle failure. The Hertzian fracture model (HFM) of Zhang et al. (1990), one of the most widely used granular micromechanical models, was developed to characterize the effects of porosity, φ, and grain radius, R, on the critical pressure required for grain crushing under hydrostatic loading, P^*. This model is predicated on the assumption that microcracks initiate from stress concentrations at the grain contacts and propagate with the progressively larger load, radiating from the grain contact to form a Hertzian fracture. Given the microstructure of our high-porosity samples and the deformation features they developed under uniaxial compression (Figure 2a), a grain-based micromechanical model may be more suitable than a pore-based model to test our high-porosity UCS data against. By analogy with Zhang et al. (1990), we use the following strength-dependent empirical relationship,

$$\sigma_u \propto \Omega(R)\left(\frac{1}{\sqrt{\varphi}}\right)^3 \quad (2)$$

where Ω is a constant that is a function of K_{IC} and the elastic properties of the solid and varies with R.

In Figure 3 we present the fit results obtained using Equations 1 and 2 with $K_{IC} = 0.7$ MPa.m$^{1/2}$ and $l_1(\varphi)$ replacing r in Equation 1, for the four different grain radii tested. In general, we find that at relatively low porosity, the prediction of the PECM is in good agreement with our experimental results (Figure 3). At relatively high porosity, we find a transition in the form of the data, such that it is less consistent with the PECM result and is better predicted by the HFM functional form. For each mean grain radius tested, we extract the porosity at which the data apparently crossover from one model to the other, which we refer to as the microstructural threshold for the change in the deformation micromechanism, CO (Figure 3).

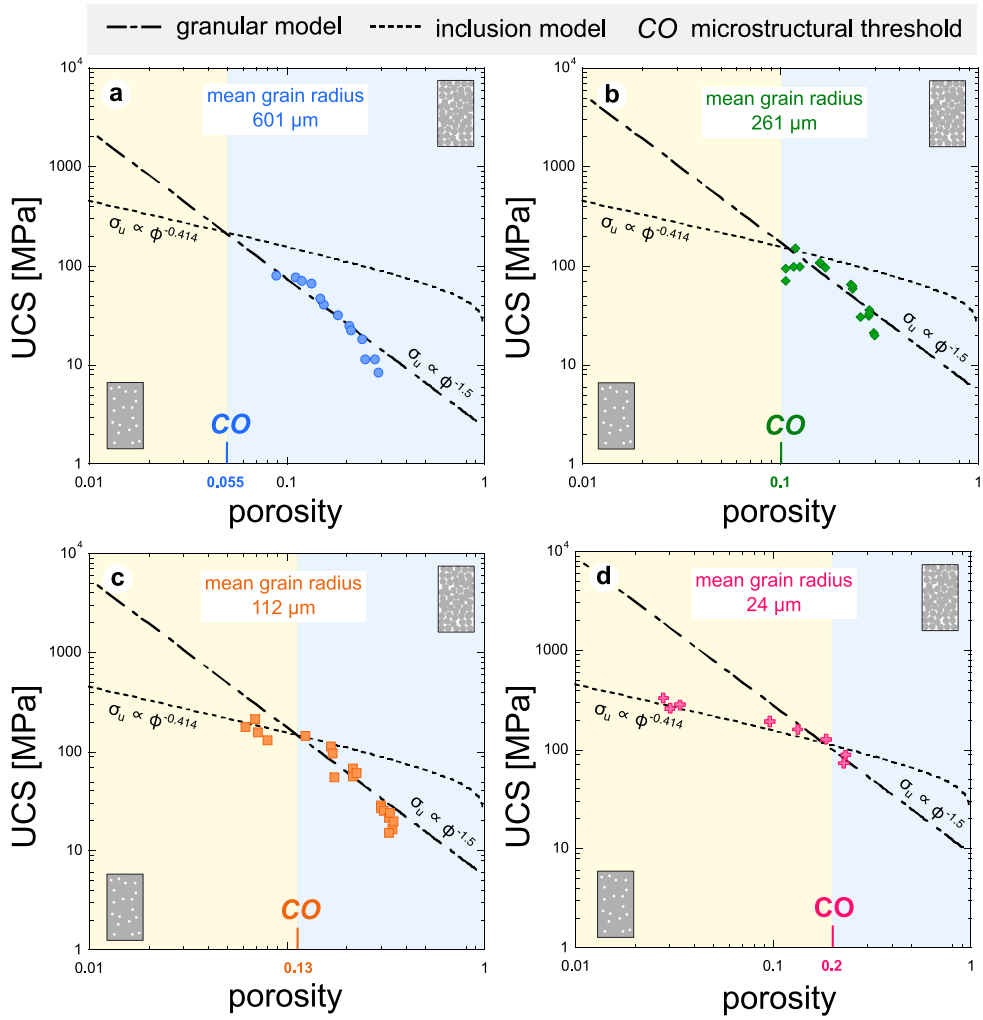

Figure 3. Experimental results for uniaxial compressive strength for (a) $R = 600$ μm, (b) $R = 260$ μm, (c) $R = 112$ μm, and (d) $R = 24$ μm compared with theoretical predictions of the pore-emanated crack model (Equation 1; Sammis & Ashby, 1986) and the empirical relation (Equation 2) derived by analogy with the Hertzian fracture model (Zhang et al., 1990). The blue and yellow areas respectively delimit the range of porosity for which the predictions of the empirical granular relation (Equation 2) and of the pore-emanated crack model are in agreement with the experimental data. The separation between these area represents the transition from one model to the other and marks a change in the pivot of dependence on porosity from an exponent of −0.414 to one of −1.5 (as indicated on the corresponding fitted lines). For each mean grain radius, the porosity at this crossover (CO) was identified.

5. Microstructural Attributes and Failure Micromechanisms

Heterogeneous materials such as natural crustal rocks demonstrate a wide variety of microstructures, from relatively simple (e.g., monomineralic and well-sorted sandstones) to relatively complex (e.g., polymineralic and poorly sorted sandstones). The ultimate goal of models for material strength is to account for a range of microstructural complexity via relatively simple-to-measure properties. Geometrically speaking, the two-phase synthetic rocks we use here represent a relatively simple system, but one which directly replicates the microstructural evolution exhibited during the diagenesis or induration of clastic rocks. Namely, the viscous sintering mechanism used to produce our samples results in a reduction of porosity via the in-pore accumulation of material at particle-particle necks, and ultimately at low porosities, the occlusion of isolated pores in a solid matrix. Under uniaxial compression, we observe that the microscopic damage is directly related to the endmember—granular or non-granular—that best describes the specific sample (Figure 2). We find that the empirical relation derived from the HFM (Equation 2) well describes our UCS data at high porosities, whereas the PECM (Equation 1) well describes the data at low porosities. This is consistent with the microstructural foundations of those two models,

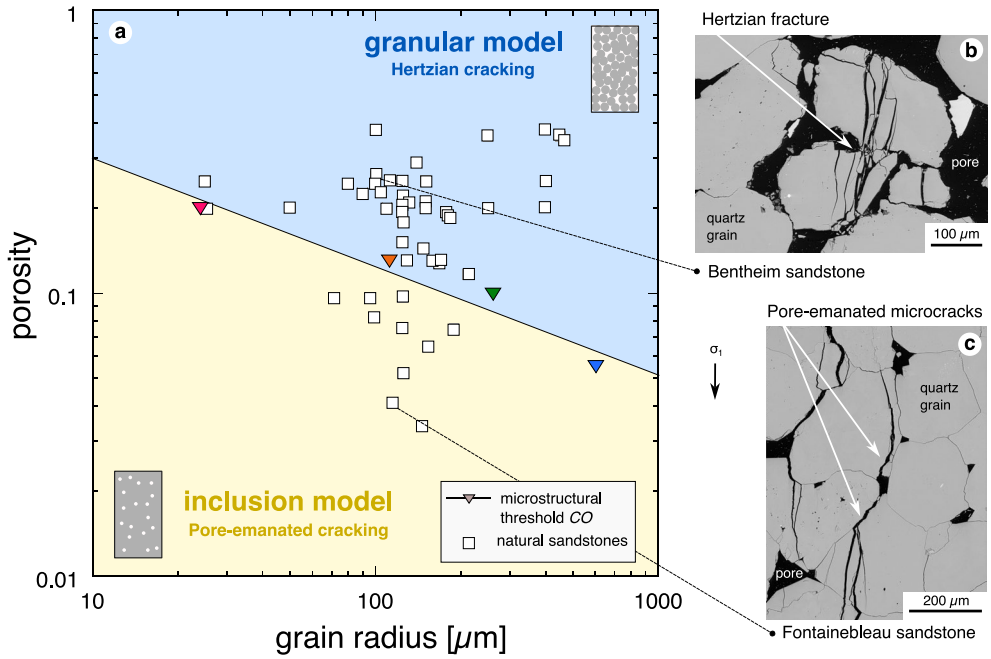

Figure 4. (a) Regime plot of the micromechanism of failure under uniaxial compression as a function of porosity and mean grain radius of the rock. The blue and yellow areas respectively delimit the range of porosity and grain size for which the empirical granular relation (Equation 2) and the inclusion model provide an accurate prediction for the experimental data. These regions are separated by the linear fit to the crossover porosity values identified using our experimental results (see Figure 3). Insights into the microstructure of (b) a sample of Fontainebleau sandstone with a porosity of 0.04 and mean grain radius of 125 μm and (c) a sample of Bentheim sandstone with a porosity of 0.24 and mean grain radius of 97 μm deformed under uniaxial compression up to the peak stress were obtained using the scanning electron microscope. As expected from the regime plot, pore-emanated microcracks were found in Fontainebleau sandstone whereas Hertzian fractures at the grain contacts were observed in Bentheim sandstone.

respectively. Moreover, our microstructural data show differences in the spatial distribution of grain-scale damage in high-porosity and low-porosity samples: whilst a strong stress-induced anisotropy is observed at low porosity, intragranular crack growth in high-porosity samples appear more isotropic (Figure 2). This is in agreement with the results of Wu et al. (2000) who used stereological techniques to quantify stress-induced damage in several rocks deformed in the brittle regime. For sandstone, Wu et al. (2000) found a significant anisotropy in Darley Dale sandstone (with an initial porosity of 0.13) and no significant anisotropy in deformed Berea sandstone (with an initial porosity of 0.21). Such an observation supports the idea to use the PECM, which predicts anisotropic deformation (Paterson & Wong, 2005), at low-porosity but a granular model similar to the HFM at high-porosity. In sedimentary settings, such difference in stress-induced anisotropy could result in differences in hydraulic properties, with the development of permeability anisotropy in low-porosity sandstones but not in high-porosity sandstones, and therefore have critical implications for reservoir and aquifer evolution.

The transition between granular and non-granular state occurs progressively during viscous sintering and densification during sedimentary diagenesis (Blair et al., 1993; Worden & Burley, 2009). Nevertheless, for a given grain radius, we find discrete porosity values for the crossover from the granular to non-granular regime (Figure 3). For a fixed grain radius, the microstructural threshold corresponds to the porosity at which the granular model prediction is no longer valid and that the PECM accurately describes the experimental UCS data. A similar crossover point was found to control hydraulic properties such as permeability (Wadsworth et al., 2017). In Figure 4, we plot our microstructural threshold values, CO, in a graph of porosity against grain radius. This plot demarks the two failure regimes and can be used to estimate which failure micromechanism may be expected and which model should therefore be used. The data for the microstructural threshold CO are well described by an empirical power law $CO = pR^q$ where we find that $p = 0.726$ and $q = -0.382$ when R is in μm. This power law divides the porosity-grain radius space in two: at low porosity-low grain radius, the predicted failure micromechanism is pore-emanated cracking and at high porosity-high grain radius, it is Hertzian cracking. By extrapolation, the porosity values that correspond to the microstructural threshold are predicted to go over the range of initial

packing porosities observed in sediment settings, 0.4–0.5 (Graton & Fraser, 1935), when the grain radius falls below 2–4 μm. Therefore, for rocks with a mean grain radius below 4 μm, our regime diagram predicts that failure under uniaxial loading would always occur by pore-emanating cracking.

By compiling data from the literature for the porosity and mean grain radius of natural sandstones with our data in Figure 4, several observations can be made. (a) At 120 μm, a length at or close to the mean grain radius of many of the natural sandstones, the transition from grain crushing to pore-emanating cracking is predicted at a porosity of ∼0.11. (b) When considering porosity and grain radius only, the expected failure micromechanism for many of the natural sandstones is grain crushing. To test whether our model predictions are valid for natural sandstones, we performed additional UCS tests on Fontainebleau (porosity of 0.04) and Bentheim sandstone (porosity of 0.25) in which we stopped deformation immediately prior to macroscopic failure and unloaded the samples for microstructural interrogation. SEM images of these samples are provided on Figure 4 and show that the pore-emanating microcracks and grain-to-grain contact microcracks are observed in the low- and high-porosity sandstones, respectively, in agreement with the predictions from our regime plot. At porosity and grain size values closer to the threshold defined, we speculate that deformation features might get more complex and involve a mix of crushed grains and pore cracks in various proportions. Indeed, Wong (1990) highlighted that brittle failure likely involves complex mechanisms such as grain crushing which are not captured by the PECM (Sammis & Ashby, 1986). In addition, occurrences of isolated clusters of Hertzian fractures and intragranular crack arrays were reported in natural sandstones deformed in the brittle regime (Menéndez et al., 1996; Wu et al., 2000). However, grain crushing is not generally reported as the dominant micromechanism of deformation for sandstones under uniaxial loading (Baud et al., 2014). One reason for this might be the lack of microstructural data for samples deformed past the onset of inelastic deformation but before macroscopic failure. The importance of other microstructural attributes such as cement content, not considered here, should also be taken into account. Indeed, cement, even in small quantities, can significantly increase rock strength (Yin & Dvorkin, 1994) and, if located at grain contacts, could alleviate the stress concentration and therefore inhibit Hertzian cracking (Menéndez et al., 1996). Moreover, Saidi et al. (2003) reported that cementation influences the grain size sensitivity of strength: when the cement content is >20–30 vol.%, the strength of their synthetic samples did not depend on grain size. Increasing the cement content, material is deposited at the grain-to-grain contacts and the microstructure progressively evolves to become non-granular so that strength no longer scales with grain size but with pore size, similar to the result we report here.

6. Conclusions

The use of sintered glass bead samples allowed us to investigate the influence of pore-space topology and grain size on the micromechanics of compressive failure. An advantage of the synthetic samples is that they are simplified two-phases materials and suitable analogs, mechanically and microstructurally, for crustal rocks (Carbillet et al., 2021). Our mechanical and microstructural data support our hypothesis that, as the microstructure transitions from a granular to a non-granular state, the mechanism for failure at the grain-scale evolves from Hertzian cracking to pore-emanated cracking. We define a threshold for this microstructural transition, which depends on porosity and grain size, whereat the micromechanical model that best describes the mechanical behavior changes. Because crustal rocks span the whole range of microstructures between the granular and non-granular endmembers, our results have applications not only for natural sandstones but also for other rocks such as tuffs (Zhu et al., 2011). Our approach can be used to provide accurate strength estimations for natural rocks with known porosity and grain size. To assist those studying the mechanical behavior of clastic rocks, we provide a regime plot that indicates the type of micromechanical model—inclusion or granular—may be more suitable to model strength for a given porosity and grain size (Figure 4).

Data Availability Statement

The data supporting the conclusions of this study are available at Carbillet (2023).

Acknowledgments
The coauthors thank John Browning and an anonymous reviewer for their valuable reviews. This paper has benefited from discussions with Jérôme Fortin, Mai-linh Doan, and Jérémie Vasseur. We also thank Thierry Reuschlé, Bertrand Renaudie, Christophe Nevado, and Gilles Morvan. The first author acknowledges funding from the Doctoral School at the University of Strasbourg. M.J. Heap acknowledges support from the Institut Universitaire de France (IUF).

References

Baud, P., Exner, U., Lommatzsch, M., Reuschlé, T., & Wong, T. (2017). Mechanical behavior, failure mode, and transport properties in a porous carbonate. *Journal of Geophysical Research: Solid Earth*, *122*(9), 7363–7387. https://doi.org/10.1002/2017JB014060

Baud, P., Wong, T., & Zhu, W. (2014). Effects of porosity and crack density on the compressive strength of rocks. *International Journal of Rock Mechanics and Mining Sciences*, *67*, 202–211. https://doi.org/10.1016/j.ijrmms.2013.08.031

Blair, S. C., Berge, P. A., & Berryman, J. G. (1993). Two-point correlation functions to characterize microgeometry and estimate permeabilities of synthetic and natural sandstones. https://doi.org/10.2172/10182383

Carbillet, L. (2023). Mechanical and microstructural data for the manuscript "Microstructural controls on the uniaxial compressive strength of porous rocks through the granular to non-granular transition" [Dataset]. Figshare. https://doi.org/10.6084/m9.figshare.23058920.v2

Carbillet, L., Heap, M. J., Baud, P., Wadsworth, F. B., & Reuschlé, T. (2021). Mechanical compaction of crustal analogs made of sintered glass beads: The influence of porosity and grain size. *Journal of Geophysical Research: Solid Earth*, *126*(4), e2020JB021321. https://doi.org/10.1029/2020jb021321

Chang, C., Zoback, M. D., & Khaksar, A. (2006). Empirical relations between rock strength and physical properties in sedimentary rocks. *Journal of Petroleum Science and Engineering*, *51*(3–4), 223–237. https://doi.org/10.1016/j.petrol.2006.01.003

Doyen, P. M. (1988). Permeability, conductivity, and pore geometry of sandstone. *Journal of Geophysical Research*, *93*(B7), 7729–7740. https://doi.org/10.1029/JB093iB07p07729

Graton, L. C., & Fraser, H. J. (1935). Systematic packing of spheres: With particular relation to porosity and permeability. *The Journal of Geology*, *43*(8, Part 1), 785–909. https://doi.org/10.1086/624386

Griffiths, L., Heap, M. J., Xu, T., Chen, C. F., & Baud, P. (2017). The influence of pore geometry and orientation on the strength and stiffness of porous rock. *Journal of Structural Geology*, *96*, 149–160. https://doi.org/10.1016/J.JSG.2017.02.006

Guéguen, Y., & Boutéca, M. (2004). *Mechanics of fluid saturated rocks*. Elsevier Academic Press. Retrieved from https://books.google.fr/books?hl=en&lr=&id=_FVt_dgDB-IC&oi=fnd&pg=PP1&dq=guéguen+yves&ots=sUcO2Nn_qz&sig=oyKs8e5n7uwAfyrcWyr9Ge6BI-Sw#v=onepage&q=guéguenyves&f=false

Kemeny, J. M., & Cook, N. G. W. (1991). Micromechanics of deformation in rocks. In S. P. Shah (Ed.), *Toughening mechanisms in quasi-brittle materials* (pp. 155–188). Springer Netherlands. https://doi.org/10.1007/978-94-011-3388-3_10

McBeck, J., Mair, K., & Renard, F. (2019). How porosity controls macroscopic failure via propagating fractures and percolating force chains in porous granular rocks. *Journal of Geophysical Research: Solid Earth*, *124*(9), 9920–9939. https://doi.org/10.1029/2019JB017825

Menéndez, B., Zhu, W., & Wong, T. (1996). Micromechanics of brittle faulting and cataclastic flow in Berea sandstone. *Journal of Structural Geology*, *18*(1), 1–16. https://doi.org/10.1016/0191-8141(95)00076-P

Paterson, M. S., & Wong, T. (2005). *Experimental rock deformation: The brittle field* (2nd ed.). Springer Verlag.

Peng, J., Wong, L. N. Y., & Teh, C. I. (2017). Influence of grain size heterogeneity on strength and microcracking behavior of crystalline rocks. *Journal of Geophysical Research: Solid Earth*, *122*(2), 1054–1073. https://doi.org/10.1002/2016JB013469

Saidi, F., Bernabé, Y., & Reuschlé, T. (2003). The mechanical behavior of synthetic, poorly consolidated granular rock under uniaxial compression. *Tectonophysics*, *370*(1–4), 105–120. https://doi.org/10.1016/S0040-1951(03)00180-X

Sammis, C. G., & Ashby, M. F. (1986). The failure of brittle porous solids under compressive stress states. *Acta Metallurgica*, *34*(3), 511–526. https://doi.org/10.1016/0001-6160(86)90087-8

Scholtès, L., & Donzé, F. V. (2013). A DEM model for soft and hard rocks: Role of grain interlocking on strength. *Journal of the Mechanics and Physics of Solids*, *61*(2), 352–369. https://doi.org/10.1016/J.JMPS.2012.10.005

Torquato, S. (2002). *Random heterogeneous materials: Microstructure and macroscopic properties*. Springer.

Vasseur, J., Wadsworth, F. B., Heap, M. J., Main, I. G., Lavallée, Y., & Dingwell, D. B. (2017). Does an inter-flaw length control the accuracy of rupture forecasting in geological materials? *Earth and Planetary Science Letters*, *475*, 181–189. https://doi.org/10.1016/J.EPSL.2017.07.011

Vasseur, J., Wadsworth, F. B., Lavallée, Y., Hess, K.-U., & Dingwell, D. B. (2013). Volcanic sintering: Timescales of viscous densification and strength recovery. *Geophysical Research Letters*, *40*(21), 5658–5664. https://doi.org/10.1002/2013GL058105

Wadsworth, F. B., Vasseur, J., Llewellin, E. W., Dobson, K. J., Colombier, M., Von Aulock, F. W., et al. (2017). Topological inversions in coalescing granular media control fluid-flow regimes. *Physical Review E*, *96*(3), 33113. https://doi.org/10.1103/PhysRevE.96.033113

Wadsworth, F. B., Vasseur, J., Llewellin, E. W., Schauroth, J., Dobson, K. J., Scheu, B., & Dingwell, D. B. (2016). Sintering of viscous droplets under surface tension. *Proceedings of the Royal Society A: Mathematical, Physical and Engineering Sciences*, *472*(2188), 20150780. https://doi.org/10.1098/rspa.2015.0780

Wong, T. (1990). *Mechanical compaction and the brittle-ductile transition in porous sandstones* (Vol. 54, pp. 111–122). Geological Society Special Publication. https://doi.org/10.1144/GSL.SP.1990.054.01.12

Wong, T., & Baud, P. (2012). The brittle-ductile transition in porous rock: A review. *Journal of Structural Geology*, *44*, 25–53. https://doi.org/10.1016/j.jsg.2012.07.010

Worden, R. H., & Burley, S. D. (2009). Sandstone diagenesis: The evolution of sand to stone. *Sandstone Diagenesis*, 1–44. https://doi.org/10.1002/9781444304459

Wu, X. Y., Baud, P., & Wong, T. F. (2000). Micromechanics of compressive failure and spatial evolution of anisotropic damage in Darley Dale sandstone. *International Journal of Rock Mechanics and Mining Sciences*, *37*(1–2), 143–160. https://doi.org/10.1016/S1365-1609(99)00093-3

Yin, H., & Dvorkin, J. (1994). Strength of cemented grains. *Geophysical Research Letters*, *21*(10), 903–906. https://doi.org/10.1029/93GL03535

Yu, Q., Zhu, W., Ranjith, P. G., & Shao, S. (2018). Numerical simulation and interpretation of the grain size effect on rock strength. *Geomechanics and Geophysics for Geo-Energy and Geo-Resources*, *4*(2), 157–173. https://doi.org/10.1007/s40948-018-0080-z

Zhang, J., Wong, T.-F., & Davis, D. M. (1990). Micromechanics of pressure-induced grain crushing in porous rocks. *Journal of Geophysical Research*, *95*(B1), 341–352. https://doi.org/10.1029/JB095iB01p00341

Zhu, W., Baud, P., Vinciguerra, S., & Wong, T. (2011). Micromechanics of brittle faulting and cataclastic flow in Alban Hills tuff. *Journal of Geophysical Research*, *116*(6), 1–23. https://doi.org/10.1029/2010JB008046

Zhu, W., Baud, P., Vinciguerra, S., & Wong, T. F. (2016). Micromechanics of brittle faulting and cataclastic flow in Mount Etna basalt. *Journal of Geophysical Research: Solid Earth*, *121*(6), 4268–4289. https://doi.org/10.1002/2016JB012826

Zhu, W., Baud, P., & Wong, T. (2010). Micromechanics of cataclastic pore collapse in limestone. *Journal of Geophysical Research*, *115*(4), B04405. https://doi.org/10.1029/2009JB006610